Acta Neuropathol (2009) 117:125–136
DOI 10.1007/s00401-008-0480-1

ORIGINAL PAPER

Phosphorylated TDP-43 in Alzheimer's disease and dementia with Lewy bodies

Tetsuaki Arai · Ian R. A. Mackenzie · Masato Hasegawa · Takashi Nonoka · Kazhuhiro Niizato · Kuniaki Tsuchiya · Shuji Iritani · Mitsumoto Onaya · Haruhiko Akiyama

Received: 5 December 2008 / Revised: 29 December 2008 / Accepted: 29 December 2008 / Published online: 13 January 2009

Abstract Phosphorylated and proteolytically cleaved TDP-43 is a major component of the ubiquitin-positive inclusions in the most common pathological subtype of frontotemporal lobar degeneration (FTLD-U). Intracellular accumulation of TDP-43 is observed in a subpopulation of patients with other dementia disorders, including Alzheimer's disease (AD) and dementia with Lewy bodies (DLB). However, the pathological significance of TDP-43 pathology in these disorders is unknown, since biochemical features of the TDP-43 accumulated in AD and DLB brains, especially its phosphorylation sites and pattern of fragmentation, are still unclear. To address these issues, we performed immunohistochemical and biochemical analyses of AD and DLB cases, using phosphorylation-dependent anti-TDP-43 antibodies. We found a higher frequency of pathological TDP-43 in AD (36–56%) and in DLB (53–60%) than previously reported. Of the TDP-43-positive cases, about 20–30% showed neocortical TDP-43 pathology resembling the FTLD-U subtype associated with progranulin gene (*PGRN*) mutations. Immunoblot analyses of the sarkosyl-insoluble fraction from cases with neocortical TDP-43 pathology showed intense staining of several low-molecular-weight bands, corresponding to C-terminal fragments of TDP-43. Interestingly, the band pattern of these C-terminal fragments in AD and DLB also corresponds to that previously observed in the FTLD-U subtype associated with *PGRN* mutations. These results suggest that the morphological and biochemical features of TDP-43 pathology are common between AD or DLB and a specific subtype of FTLD-U. There may be genetic factors, such as mutations or genetic variants of *PGRN* underlying the co-occurrence of abnormal deposition of TDP-43, tau and α-synuclein.

Keywords Phosphorylation · Fragmentation · Frontotemporal lobar degeneration · Progranulin · Tau · Alpha-synuclein · TDP-43

T. Arai (✉) · H. Akiyama
Department of Psychogeriatrics,
Tokyo Institute of Psychiatry,
Tokyo Metropolitan Organization for Medical Research,
2-1-8 Kamikitazawa, Setagaya-ku, Tokyo 156-8585, Japan
e-mail: arai@prit.go.jp

I. R. A. Mackenzie
Department of Pathology,
Vancouver General Hospital, 855 West 12th Avenue,
Vancouver, BC V5Z 1M9, Canada

M. Hasegawa · T. Nonoka
Department of Molecular Neurobiology,
Tokyo Institute of Psychiatry,
Tokyo Metropolitan Organization for Medical Research,
2-1-8 Kamikitazawa, Setagaya-ku,
Tokyo 156-8585, Japan

K. Niizato
Department of Psychiatry,
Tokyo Metropolitan Matsuzawa Hospital,
2-1-1 Kamikitazawa, Setagaya-ku, Tokyo 156-0057, Japan

K. Tsuchiya
Department of Laboratory Medicine and Pathology,
Tokyo Metropolitan Matsuzawa Hospital, 2-1-1 Kamikitazawa,
Setagaya-ku, Tokyo 156-0057, Japan

S. Iritani
Department of Psychiatry,
Nagoya University Graduate School of Medicine,
Nagoya, Aichi 466-8550, Japan

M. Onaya
Department of Neuropsychiatry,
National Shimofusa Mental Hospital, Chiba 266-0007, Japan

Introduction

TAR DNA-binding protein of M_r 43 kDa (TDP-43) is a major component of the tau-negative and ubiquitin-positive inclusions that characterize the most common pathological subtype of frontotemporal lobar degeneration (FTLD-U) and amyotrophic lateral sclerosis (ALS) [2, 9, 24, 31, 32, 38]. Several genes and chromosomal loci, including the progranulin gene (*PGRN*) [4, 8], valosin-containing protein gene (*VCP*) [42] and an unidentified gene at chromosome 9p [28, 41], have been reported to be associated with familial forms of FTLD-U. Recent findings of various missense mutations of TDP-43 gene (*TARDBP*) in familial and sporadic ALS cases prove the essential role of abnormal TDP-43 in neurodegeneration [12, 20, 37, 40, 43]. These disorders are now collectively referred to as TDP-43 proteinopathies [2, 9, 31, 32].

Ubiquitin- and TDP-43-positive pathological inclusions found in FTLD-U include neuronal cytoplasmic inclusions (NCIs), dystrophic neurites (DNs), neuronal intranuclear inclusions (NIIs), and glial cytoplasmic inclusions [2, 25, 26, 32, 35]. Based on the cerebral ubiquitin immunohistochemistry, FTLD-U was classified into three subtypes by Sampathu et al. [35] and Mackenzie et al. [25]. Unfortunately, the numbering schemes used in these two systems do not match. Type 1 by Sampathu et al. or Type 2 by Mackenzie et al. is characterized by DNs with few NCIs and no NIIs. Type 2 by Sampathu et al. or Type 3 by Mackenzie et al. has numerous NCIs with few DNs and no NIIs. Type 3 by Sampathu et al. or Type 1 by Mackenzie et al. has numerous NCIs and DNs and occasional NIIs. This is the pattern found in all cases of FTD caused by mutations in *PGRN* [7, 25]. Recently, Cairns et al. [7] drew these two systems together into a unified scheme, and added familial FTLD-U with *VCP* mutations as Type 4, which has numerous NIIs and DNs with few NCIs. Since they adopted the numbering system by Sampathu et al. in their consensus paper, we will use that for the rest of this paper.

Biochemical analyses of the detergent-insoluble fraction extracted from brains of patients afflicted with FTLD-U showed that TDP-43 accumulated in these pathological structures is composed of abnormal C-terminal fragments that are phosphorylated and ubiquitinated [2, 32]. Using antibodies specific for phosphorylated TDP-43 (pTDP-43), made by ourselves, we previously identified several phosphorylation sites in the C-terminal region of the TDP-43 that accumulates in FTLD-U brains [14]. Furthermore, we found a close relationship between the pathological subtypes of FTLD-U and the immunoblot pattern of phosphorylated C-terminal fragments of TDP-43, suggesting that proteolytic processing may be crucial in TDP-43 proteinopathy [14].

Recently, immunohistochemical examination, using commercially available phosphorylation-independent anti-TDP-43 antibodies, has demonstrated abnormal intracellular accumulation of TDP-43 in neurodegenerative disorders other than FTLD-U and ALS. These include Alzheimer's disease (AD), dementia with Lewy bodies (DLB), Pick's disease, hippocampal sclerosis, corticobasal degeneration, Huntington disease and argyrophilic grain disease [1, 11, 15, 17, 19, 23, 30, 36, 39]. However, the pathological significance of TDP-43 accumulation in these disorders is unclear, since it takes place only in a subpopulation of the patients with most of these disorders. Moreover, although the morphology of the TDP-43 positive structures has been described, the biochemical features of accumulated TDP-43, especially its phosphorylation sites and fragmentation, are still unclear in these disorders. To address these issues, in the present study, we performed detailed immunohistochemical and biochemical analyses of TDP-43 in cases of AD and DLB, using our phosphorylation-dependent anti-TDP-43 antibodies. We find a relatively higher frequency of TDP-43 deposition in AD and DLB than previously reported. When TDP-43 pathology occurs in the neocortex of cases with AD and DLB, the pattern is Type 3. In these cases, the accumulated TDP-43 demonstrates abnormal C-terminal phosphorylation and fragmentation. These results suggest the presence of a common mechanism underlying the abnormal processing and accumulation of TDP-43 in AD, DLB and a specific subtype of FTLD-U.

Materials and methods

Materials

We studied two independent series of cases (Table 1). The first was comprised of 53 AD cases and 15 DLB cases from the institutional collections at the Department of Psychogeriatrics, Tokyo Institute of Psychiatry in Japan. The second series included 25 AD cases and 10 DLB cases from the Canadian Collaborative Cohort of Related Dementia (ACCORD) study, a well-characterized memory clinic population, prospectively followed to death [10]. The second series provided validation of the findings from the first series, included examination of some additional neuroanatomical regions not available in the first series and tested whether similar results could be obtained by using more traditional immunohistochemical methodology.

Neuropathological diagnoses of AD and DLB were made in accordance with published guidelines [27, 33] for both series. Two cases from the first series and one case from the second series had little AD pathology, corresponding to the pure form of diffuse Lewy body disease (DLBD) [21].

Table 1 Demographics and pathology of all cases employed in this study

	Alzheimer's disease						Dementia with Lewy bodies					
	First series ($N = 53$)			Second series ($N = 25$)			First series ($N = 15$)			Second series ($N = 10$)		
	TDP-43 positive	TDP-43 negative	*P* value	TDP-43 positive	TDP-43 negative	*P* value	TDP-43 positive	TDP-43 negative	*P* value	TDP-43 positive	TDP-43 negative	*P* value
Number of cases (%)	19 (36%)	34 (64%)		14 (56%)	11 (44%)		8 (53%)	7 (47%)		6 (60%)	4 (40%)	
Mean age at death ± SD (years)	82.8 ± 7.5	78.8 ± 10.7	0.16	81.2 ± 7.0	72.7 ± 9.2	0.015*	73.5 ± 12.8	81.7 ± 6.5	0.15	76.3 ± 7.4	71.0 ± 9.5	0.35
Sex, M:F	11:8	20:14	0.95	8:6	5:6	0.56	6:2	5:2	>0.99	4:2	3:1	>0.99
Median Braak NFT stage (25th, 75th percentile)	5 (5.0, 6.0)	5 (4.0, 5.0)	0.027*	6 (6.0, 6.0)	6 (6.0, 6.0)	0.7	4 (3.0, 6.0)	4 (3.25, 4.0)	0.54	4.5 (2.0, 6.0)	6 (6.0, 6.0)	0.11
Brain weight ± SD (g)	1,117 ± 162	1,116 ± 137	0.98	NA	NA		1,123 ± 151	1,144 ± 146	0.79	NA	NA	

Immunohistochemistry

For the first series, small blocks of brain were dissected at autopsy and fixed in 4% paraformaldehyde (PFA) in 0.1 M phosphate buffer (pH 7.4) for 2 days. Following the cryoprotection in 15% sucrose in 0.01 M phosphate-buffered saline (PBS, pH 7.4), blocks were cut on a freezing microtome at 30 µm thickness. The free floating sections were incubated with 0.5% H_2O_2 for 30 min to eliminate endogenous peroxidase activity in the tissue. After washing with PBS containing 0.3% Triton X-100 (Tx-PBS) for 30 min, sections were blocked with 10% normal serum, and then incubated with the primary antibody for 72 h in the cold. Following treatment with the appropriate secondary antibody, labeling was detected using the avidin–biotinylated HRP complex (ABC) system (Vector Laboratories, Burlingame, CA) coupled with a diaminobenzidine (DAB) reaction to yield a brown precipitate, or with a DAB reaction intensified with nickel ammonium sulfate to yield a dark purple precipitate, as previously described [2, 3, 13, 14]. For the second series, immunohistochemistry was performed on 5-µm-thick sections of formalin-fixed, paraffin-embedded tissue, using the Ventana BenchMark® XT automated staining system (Ventana, Tuscon, AZ), as previously described [25]. Prior to immunostaining, sections underwent microwave antigen retrieval for 13 min in citrate buffer, pH 6.0. Immunoreactions were developed with aminoethylcarbizole (AEC).

In the first series, the presence and severity of pTDP-43 immunoreactivity was assessed in amygdala (where available), hippocampus, entorhinal cortex and temporal neocortex. More extensive anatomical sampling was available in the second series allowing pathology to be assessed in the amygdala, hippocampus, entorhinal cortex, cingulate gyrus, temporal neocortex, frontal neocortex and parietal neocortex. pTDP-43 pathology was semiquantitatively scored based on a five-point grading scale (−, none; ±, rare; +, mild; ++, moderate; +++, severe). The primary antibodies used in this study and their dilutions are summarized in Table 2. Only pTDP-43-specific antibodies (pS409/410 and pS403/404) were employed in the first series, while both phosphorylation-independent commercial anti-TDP-43 antibody and pTDP-43-specific antibodies were employed in the second series. In the second series, all the same cases were stained with both antibodies but the pTDP-43-specific antibodies often stained a greater amount of pathology.

Statistical analyses

Unpaired Student's *t* tests were used to analyze differences between groups for age and brain weights, whereas the Braak stage score was analyzed with Mann–Whitney

Table 2 Antibodies used in this study

Antibody	Type	Source	Dilution
Phosphorylation-independent anti-TDP-43			
Anti-TDP-43	Rabbit polyclonal (affinity purified)	ProteinTech, Chicago, IL	1:1,000 (IB, IHC-P)
Phosphorylation-dependent anti-TDP-43			
pS409/410	Rabbit serum	[a]	1:1,000 (IB, IHC-P), 1:10,000 (IHC-F), 1:5,000 (IF)
pS403/404	Rabbit serum	[a]	1:1,000 (IB, IHC-P), 1:10,000 (IHC-F), 1:5,000 (IF)
Anti-tau			
AT8	Mouse monoclonal	Innogenetics, Gent, Belgium	1:2,000 (IHC-P), 1:100 (IF)
Anti-α-synuclein			
pα#64	Mouse monoclonal	Wako Chemical, Osaka, Japan	1:3,000 (IF)
Anti-α-synuclein	Mouse monoclonal	Invitrogen, Burlington, ON, Canada	1:10,000 (IHC-P)
Anti-amyloid β protein			
6F3D	Mouse monoclonal	DAKO, Mississauga, ON, Canada	1:100 (IHC-P)

IB immunoblotting, *IHC-P* immunohistochemistry in paraffin-embedded sections, *IHC-F* immunohistochemistry in free-floating sections, *IF* immunofluorescence

[a] Made by ourselves [14]

U test. χ^2 and Fisher's exact test were used to analyze the difference between groups for sex.

Confocal microscopy

For double labeling immunofluorescence for pTDP-43 and phosphorylated tau in AD or for pTDP-43 and phosphorylated α-synuclein in DLB, 4% PFA-fixed and free floating sections from the first series were used. The sections were incubated overnight at 4°C in a cocktail of pS409/410 or pS403/404 and AT8 or pα#64. After washing with Tx-PBS for 30 min, sections were incubated for 2 h at room temperature in a cocktail of Fluorescein isothiocianate (FITC)-conjugated goat anti-mouse IgG (1:100, Millipore, Temecula, CA) and tetramethylrhodamine isothiocyanate (TRITC)-conjugated goat anti-rabbit IgG (1:100, Millipore). After washing, sections were incubated in 0.1% Sudan Black B for 10 min at room temperature and washed with Tx-PBS for 30 min. Sections were coverslipped with Vectashield (Vector Laboratories) and observed with a confocal laser microscope (LSM5 PASCAL; Carl Zeiss MicroImaging gmbh, Jena, Germany).

Immunoblotting

Sarkosyl-insoluble, urea-soluble fractions were extracted from the temporal lobe of an autopsied case with no neurological abnormality as a normal control and cases with AD, DLB and FTLD-U, as previously described [13, 14]. For SDS-PAGE of the samples, 15% polyacrylamide gel was used to visualize low-molecular weight fragments of accumulated TDP-43 clearly as previously reported [14]. Proteins in the gel were then electrotransferred onto a polyvinylidene difluoride membrane (Millipore Corp., Bedford, MA). After blocking with 3% gelatin in Tris-buffered saline (20 mM Tris–HCl, pH 7.5, 500 mM NaCl), membranes were incubated overnight with pS409/410 or pS403/404. Following incubation with an appropriate biotinylated secondary antibody, labeling was detected using the ABC system coupled with a DAB reaction intensified with nickel chloride.

Results

Immunohistochemical analyses

Accumulation of phosphorylated TDP-43 in AD

As we have described previously, antibodies against pTDP-43 demonstrated abnormal structures only and did not show the diffuse nuclear staining pattern typical of normal TDP-43 [14]. The two primary antibodies (pS409/410 and pS403/404) labeled similar pathological structures with similar sensitivity. pTDP-43-positive structures were present in 36% (19/53) of the first AD series (Tables 1, 3) and in 56% (14/25) of the second AD series (Tables 1, 4) with highly variable severity and regional distribution among these cases. The frequency of pTDP-43 immunoreactivity in the two series was not significantly different ($\chi^2 = 2.826$; 1 *df*; $P = 0.093$). pTDP-43-positive NCIs and DNs were variably present in the amygdala, hippocampus, parahippocampal

Table 3 TDP-43-positive structures in the first series of Alzheimer's disease

Case no.	Age	Sex	SP (CERAD)	NFT (Braak)	Amyg	DG	CA4	CA2/3	CA1	Sub	EC	Temp	TDP-43 path
F-AD1	86	M	NA	NA	+++	NA	NA	NA	NA	++	+++	+++	Diffuse
F-AD2	85	F	C	V	NA	+++	++	++	++	+	+++	+++	Diffuse
F-AD3	80	F	C	V	NA	++	+	+	++	++	+++	+++	Diffuse
F-AD4	67	F	C	VI	NA	±	−	−	+	++	+++	+++	Diffuse
F-AD5	82	M	NA	NA	NA	++	−	±	++	++	++	−	Limbic
F-AD6	85	F	C	VI	NA	+	−	±	±	+	++	−	Limbic
F-AD7	86	M	C	V	+	+	−	−	±	+	++	−	Limbic
F-AD8	86	M	NA	NA	−	−	−	−	±	+	+	−	Limbic
F-AD9	75	M	C	VI	+	+	±	±	±	+	+	±	Limbic
F-AD10	77	M	C	V	NA	NA	NA	NA	NA	++	−	−	Limbic
F-AD11	78	M	C	VI	NA	±	−	−	±	+	−	−	Limbic
F-AD12	96	M	NA	NA	NA	−	−	−	−	+	−	−	Limbic
F-AD13	91	F	C	IV	NA	−	−	−	−	+	−	−	Limbic
F-AD14	89	F	C	V	NA	−	−	−	−	+	−	−	Limbic
F-AD15	81	F	C	V	++	±	−	−	−	+	+	−	Limbic
F-AD16	93	M	C	V	NA	−	−	−	−	+	−	−	Limbic
F-AD17	75	M	C	VI	−	−	−	−	+	+	+	−	Limbic
F-AD18	89	M	C	V	+	−	−	−	−	−	+	−	Limbic
F-AD19	72	F	NA	NA	+	NA	NA	NA	NA	NA	NA	NA	NA

SP Senile plaque, *NFT* neurofibrillary tangle, *Amyg* amygdala, *DG* dentate gyrus, *Sub* subiculum, *EC* entorhinal cortex, *Temp* temporal cortex, *path* pathology, *NA* not available

−, None; ±, slight; +, mild; ++, moderate; +++, severe

Table 4 TDP-43-positive structures in the second series of Alzheimer's disease

Case no.	Age	Sex	SP (CERAD)	NFT (Braak)	Amyg	DG	CA4	CA2/3	CA1	Sub	EC	Cing	Temp	Front	Par	TDP-43 path
S-AD1	72	F	C	VI	+++	++	+	+	+++	+++	+++	+	+++	+	−	Diffuse
S-AD2	85	M	C	V	+++	+++	+++	+++	+++	+++	+++	+++	+++	++	+	Diffuse
S-AD3	84	M	C	V	+++	+++	+	++	++	+++	+++	++	+++	+++	+	Diffuse
S-AD4	89	M	C	VI	+++	++	±	+	+++	+++	+++	+	++	−	−	Diffuse
S-AD5	81	F	C	VI	+++	++	−	±	+++	+++	+++	+	++	−	−	Diffuse
S-AD6	80	M	C	VI	+++	+	±	+	+++	++	++	±	−	−	−	Limbic
S-AD7	80	F	C	VI	++	±	−	−	++	++	++	−	−	−	−	Limbic
S-AD8	89	F	C	VI	±	+	±	+	+++	+++	+	−	−	−	−	Limbic
S-AD9	84	F	C	VI	++	−	−	−	±	+	+	−	−	−	−	Limbic
S-AD10	95	M	C	VI	++	−	−	−	±	±	+	−	−	−	−	Limbic
S-AD11	74	F	C	VI	±	−	−	−	−	−	−	−	−	−	−	Amygdala
S-AD12	72	M	C	VI	±	−	−	−	−	−	−	−	−	−	−	Amygdala
S-AD13	79	M	C	VI	+	−	−	−	−	−	−	−	−	−	−	Amygdala
S-AD14	73	M	C	VI	±	−	−	−	−	−	−	−	−	−	−	Amygdala

SP Senile plaque, *NFT* neurofibrillary tangle, *Amyg* amygdala, *DG* dentate gyrus, *Sub* subiculum, *EC* entorhinal cortex, *Cing* cingulate cortex, *Temp* temporal cortex, *Front* frontal cortex, *Par* parietal cortex, *path* pathology

−, None; ±, slight; +, mild; ++, moderate; +++, severe

gyrus and neocortex (Fig. 1). In cases where the neocortex was involved, NCIs and DNs were predominantly distributed in the upper layers, most closely resembling FTLD-U type 3. Moreover, most of these cases also had a few NIIs with a lentiform shape in the dentate gyrus or the neocortex, similar to those characteristic of cases with *PGRN* mutations [26] (Fig. 1k, inset). Neurofibrillary tangle-like pTDP-43-positive structures were occasionally found in the CA1 region (Fig. 1f). Small round, short thread-like or coiled body-like structures were sometimes observed in the white

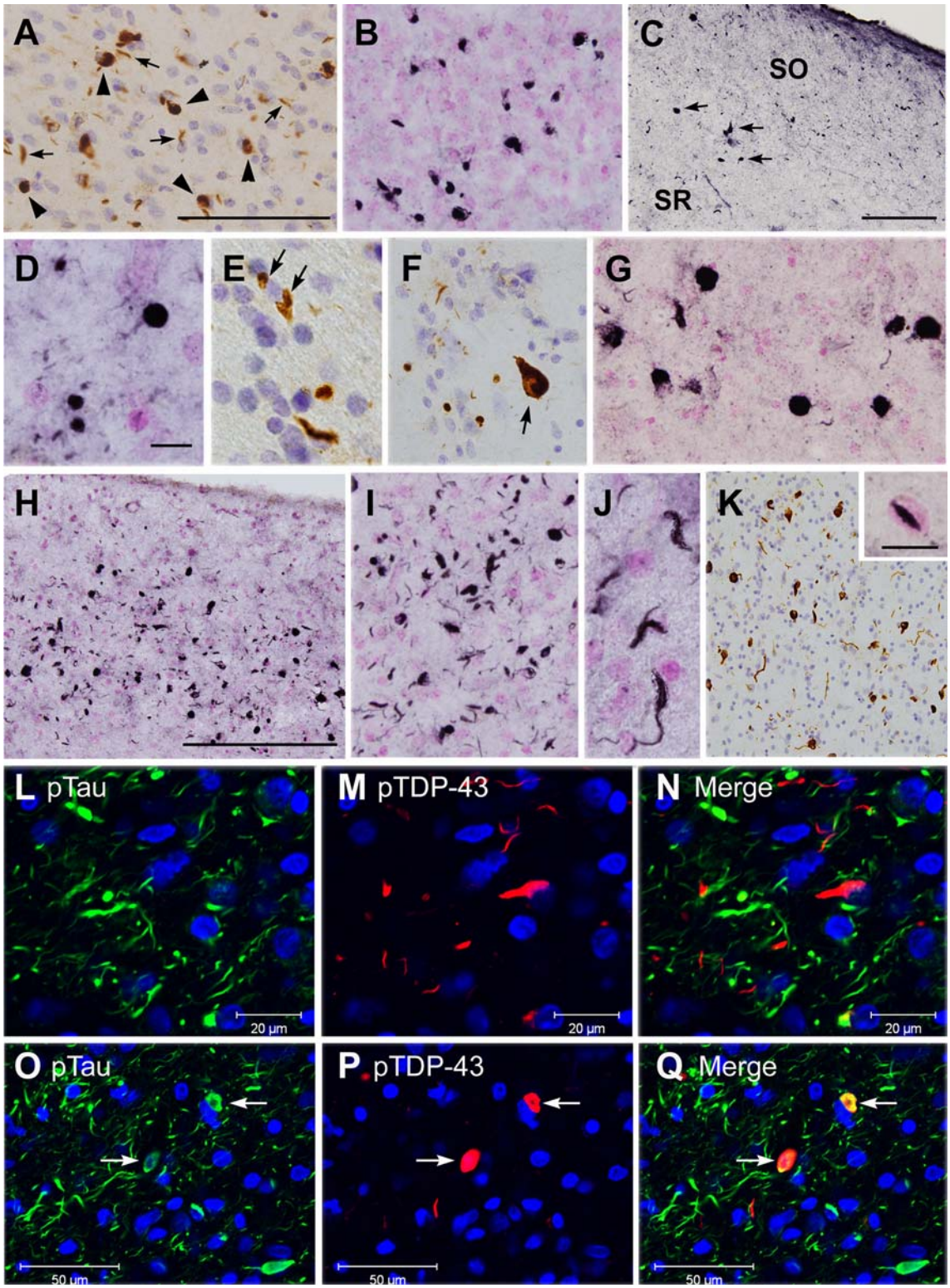

matter, including the stratum radiatum and the stratum oriens of the CA2/3 region, alveus and parahippocampal white matter. In double labeling immunofluorescence experiments, cortical tau-positive neuropil threads and TDP-43-positive dystrophic neurites were usually stained independently (Fig. 1l–n), while some neurons showed cytoplasmic inclusions immunoreactive for both markers (Fig. 1o–q).

In 19 cases with pTDP-43 immunoreactivity in the first series (Table 3), pTDP-43 pathology was largely restricted

◀ **Fig. 1** Phosphorylated TDP-43 (*pTDP-43*) positive structures in Alzheimer's disease cases with diffuse type of TDP-43 pathology. **a** Neuronal cytoplasmic inclusions (NCIs) (*arrowheads*) and dystrophic neurites (DNs) (*arrows*) in amygdala. **b** NCIs in the granule cells of the dentate gyrus. **c** NCIs in the principal layer (*arrows*) and small round or short threads-like structures in the stratum oriens (*SO*) and stratum radiatum (*SR*) of the CA2/3 region. **d** A high power view of small round or short threads-like structures in the stratum oriens of the CA2/3 region. **e** Glial cytoplasmic inclusions (*arrows*) and a small round or a short threads-like structure in the alveus of the CA1 region. **f** A neurofibrillary tangle-like structure (*arrow*), small round structures and short neurites in the principal layer of the CA1 region. **g** Large NCIs and short neurites in the subiculum. **h** Massive NCIs and DNs in the superficial layer of the entorhinal cortex. **i** A high power view of NCIs and DNs in the entorhinal cortex. **j** Glial cytoplasmic inclusions in the white matter of the parahippocampal gyrus. **k** Numerous NCIs and DNs in the superficial layer of the lateral occipitotemporal cortex. *Inset* shows a neuronal intranuclear inclusion with a lentiform shape. Double label immunofluorescence (**l–q**) demonstrates that most tau-positive neuropil threads (*green fluorescence* in **l**) and pTDP-43 positive DNs (*red fluorescence* in **m**) in the temporal neocortex are independent (**n**), while there is partial colocalization of tau and pTDP-43 in some neuronal cytoplasmic inclusions (*arrows* in **o–q**). Immunohistochemistry using primary antibodies pS403/404 (**a**, **e**, **f**, **k**) and pS409/410 (**b**, **c**, **d**, **g**, **h**, **i**, **j**). Double label immunofluorescence with anti-phosphorylated tau (AT8) and pS403/404 (**l–q**). *Scale bars* **a**, **b**, **c**, **f**, **g**, **i** 100 μm; **d**, **e**, **j**, *inset* in **k** 10 μm; **h**, **k** 200 μm

to the limbic region (amygdala, hippocampus and entorhinal cortex) in 14 cases (73.7%). This distribution of pTDP-43 pathology corresponds to the "limbic type" according to Amador-Ortiz et al. [1]. The remaining four cases (21.1%) showed more widespread lesions with numerous NCIs and DNs in the temporal neocortex; corresponding to the "diffuse type" according to Amador-Ortiz et al. [1]. Of the 14 cases with pTDP-43 immunoreactivity in the second series (Table 4), pTDP-43 pathology was found only in the amygdala in 4 cases (28.6%), showed more widespread involvement of limbic structures in 5 cases (35.7%) and extended into the cerebral neocortex in the remaining 5 cases (35.7%).There appeared to be a hierarchy to the anatomical distribution and severity of involvement that was best demonstrated in the second series (Table 4). The pathology seemed to start in the amygdala and then progress to other limbic structures before involving the neocortex. Among neocortical regions, the temporal lobe was always involved, the frontal lobe less frequently and only rarely the parietal lobe was affected.

The mean age at death was significantly higher in cases with pTDP-43 immunoreactivity in the second series ($P = 0.015$). A similar tendency was also observed in the first series, but it was not statistically significant ($P = 0.16$). The Braak NFT stage score was significantly higher in cases with pTDP-43 immunoreactivity in the first series ($P = 0.027$). This correlation could not be assessed in the second series since there was insufficient range in the Braak stage among the cases (Tables 1, 4). There were no differences in sex or brain weight between the cases with pTDP-43 immunoreactivity and those without (see Table 1).

Accumulation of phosphorylated TDP-43 in DLB

pTDP-43-positive structures were found in 53% (7/15) of the first DLB series (Tables 1, 5) and in 60% (6/10) of the second DLB series (Tables 1, 6) with variable frequency and regional distribution. There was no significant difference in the frequency of pTDP-43 immunoreactivity between the two series ($\chi^2 = 0.000$; 1 *df*; $P > 0.999$).

Figure 2 illustrates pTDP-43-positive structures observed in DLB + AD cases (a–j, m–o) and in pure DLBD cases (k, l). The morphology and anatomical distribution of the pathology was similar to that seen in the series of AD cases and the neocortical involvement again resembled FTLD-U Type 3 with a few lentiform NIIs. In double labeling confocal microscopy for pTDP-43 and phosphorylated α-synuclein in the cortex, some neurons showed cytoplasmic inclusions immunoreactive for both markers (m–o).

Of the eight cases with pTDP-43 immunoreactivity in the first DLB series (Table 5), TDP-43 pathology was

Table 5 TDP-43-positive structures in the first series of dementia with Lewy bodies

Case no.	Age	Sex	SP (CERAD)	NFT (Braak)	DLB likelihood	Pathological diagnosis	Amyg	DG	CA4	CA2/3	CA1	Sub	EC	Temp	TDP-43 path
F-DLB1	63	F	C	VI	Int.	DLB + AD	NA	+++	+	++	+	++	+++	++	Diffuse
F-DLB2	67	M	C	VI	Int.	DLB + AD	+++	+++	+	++	+	++	+++	++	Diffuse
F-DLB3	82	F	C	VI	Int.	DLB + AD	NA	+	±	+	+	++	++	+	Diffuse
F-DLB4	83	M	C	IV	High	DLB + AD	+++	+	−	+	+	++	+++	−	Limbic
F-DLB5	89	M	C	IV	High	DLB + AD	NA	−	−	+	−	+	+	−	Limbic
F-DLB6	71	M	C	IV	High	DLB + AD	NA	±	−	±	−	±	±	−	Limbic
F-DLB7	51	M	0	II	High	DLB	++	+	+	++	±	++	++	−	Limbic
F-DLB8	82	M	0	II	High	DLB	+	−	−	−	−	−	+	−	Limbic

SP Senile plaque, *NFT* neurofibrillary tangle, *Amyg* amygdala, *DG* dentate gyrus, *Sub* subiculum, *EC* entorhinal cortex, *Temp* temporal cortex, *path* pathology, *NA* not available

−, None; ±, slight; +, mild; ++, moderate; +++, severe

Table 6 TDP-43-positive structures in the second series of dementia with Lewy bodies

Case no.	Age	Sex	SP (CERAD)	NFT (Braak)	DLB likelihood	Pathological diagnosis	Amyg	DG	CA4	CA2/3	CA1	Sub	EC	Cing	Temp	Front	Par	TDP-43 path
S-DLB1	90	F	C	VI	Int.	DLB + AD	+++	–	–	–	–	+	±	–	–	–	–	Limbic
S-DLB2	79	M	C	VI	Int.	DLB + AD	++	–	–	–	–	–	±	–	–	–	–	Limbic
S-DLB3	74	M	0	II	High	DLB	+	–	–	–	–	–	–	–	–	–	–	Amygdala
S-DLB4	70	M	C	II	High	DLB	+	NA	NA	NA	NA	NA	NA	–	–	–	–	Amygdala
S-DLB5	71	M	C	III	High	DLB	±	–	–	–	–	–	–	–	–	–	–	Amygdala
S-DLB6	74	F	C	VI	Int.	DLB + AD	±	–	–	–	–	–	–	–	–	–	–	Amygdala

SP Senile plaque, *NFT* neurofibrillary tangle, *Amyg* amygdala, *DG* dentate gyrus, *Sub* subiculum, *EC* entorhinal cortex, *Cing* cingulate cortex, *Temp* temporal cortex, *Front* frontal cortex, *Par* parietal cortex, *path* pathology, *NA* not available

–, None; ±, slight; +, mild; ++, moderate; +++, severe

largely confined to limbic region in five cases (62.5%), while three cases (37.5%) revealed more widespread lesions in the temporal cortex. In the second series (Table 6), four cases (66.7%) showed slight TDP-43 pathology only in amygdala and the remaining two cases (33.3%) showed moderate to severe TDP-43 pathology in amygdala and slight to mild TDP-43 pathology in limbic region.

There were no significant differences in the mean age at death, sex and Braak NFT stage score between cases with pTDP-43 immunoreactivity and those without, in either series (see Table 1). All three cases with pure DLB had some TDP-43 pathology.

Biochemical analyses of accumulated TDP-43 in AD and DLB

Figure 3 shows immunoblot analyses of sarkosyl-insoluble, urea-soluble fractions extracted from brains of a normal control (lane 1), AD without pTDP-43 immunoreactivity (AD−, lane 2), DLB with pTDP-43 immunoreactivity (DLB+, F-DLB2, see Table 5) (lane 3), AD with pDP-43 immunoreactivity (AD+, F-AD1, see Table 3) (lane 4), FTLD-U, Type 3 (lane 5), and FTLD-U, Type 1 (lane 6). With phosphorylation-dependent antibodies specific for pS409/410 (a) and for pS403/404 (b), intense immunoreactivity throughout the gel was observed only in DLB+ (lane 3), AD+ (lane 4), FTLD-U, Type 3 (lane 5), and FTLD-U, Type 1 (lane 6). Regarding low-molecular-weight fragments, DLB+ (lane 3) and AD+ (lane 4) showed a similar pattern with three major bands at 23, 24 and 26 kDa and two minor bands at 18 and 19 kDa. Of three major bands, a 23 kDa band was the most intense, while the immunoreactivity of two minor bands at 18 and 19 kDa was similar. This band pattern corresponds to that of FTLD-U, Type 3 (see lane 5 in a, b and schematic diagram in c), previously reported by us [14]. FTLD-U with Type 1 (lane 6) showed a band pattern with two major bands at 23 and 24 kDa and two minor bands at 18 and 19 kDa, which is consistent with our previous report [14].

Discussion

In this study, we used phosphorylation-dependent anti-TDP-43 antibodies to perform detailed immunohistochemical and biochemical examination of two independent series of brains with AD and DLB. We found higher frequencies of TDP-43 pathology in AD (36–56%) and DLB (53–60%) than in previous reports [1, 16, 17, 19, 28, 36]. This may be due to the two immunohistochemical protocols we employed, one on free-floating sections and the other using an automated immunostainer for paraffin sections, are more sensitive than the methods used in previous studies. In addition, the higher frequencies found in our second series are partially explained by inclusion of examination of the amygdala, the region that appears to be most often affected by TDP-43 pathology [17].

The largely consistent observations between our two series, despite differences in the ethnic populations and source of the clinical cases, suggest that our findings are more likely to be broadly applicable to other populations of AD and DLB patients. We have also demonstrated that similar findings are attainable using various immunohistochemical methodology employed by different labs.

In immunohistochemical examinations of AD and DLB cases in the present study, phosphorylation-dependent anti-TDP-43 antibodies stained NCIs and DNs in the cerebral grey matter as previously reported [1, 16, 30, 39], and some thread-like or coiled body-like structures in the whiter matter. Regarding the distribution of TDP-43 pathology in AD, Amador-Ortiz et al. [1] first classified it into limbic and diffuse types, and indicated that limbic involvement was more common. Subsequently, Hu et al. [17] found some AD cases with TDP-43 pathology confined to the amygdala only. They suggested that the amygdala is the most susceptible

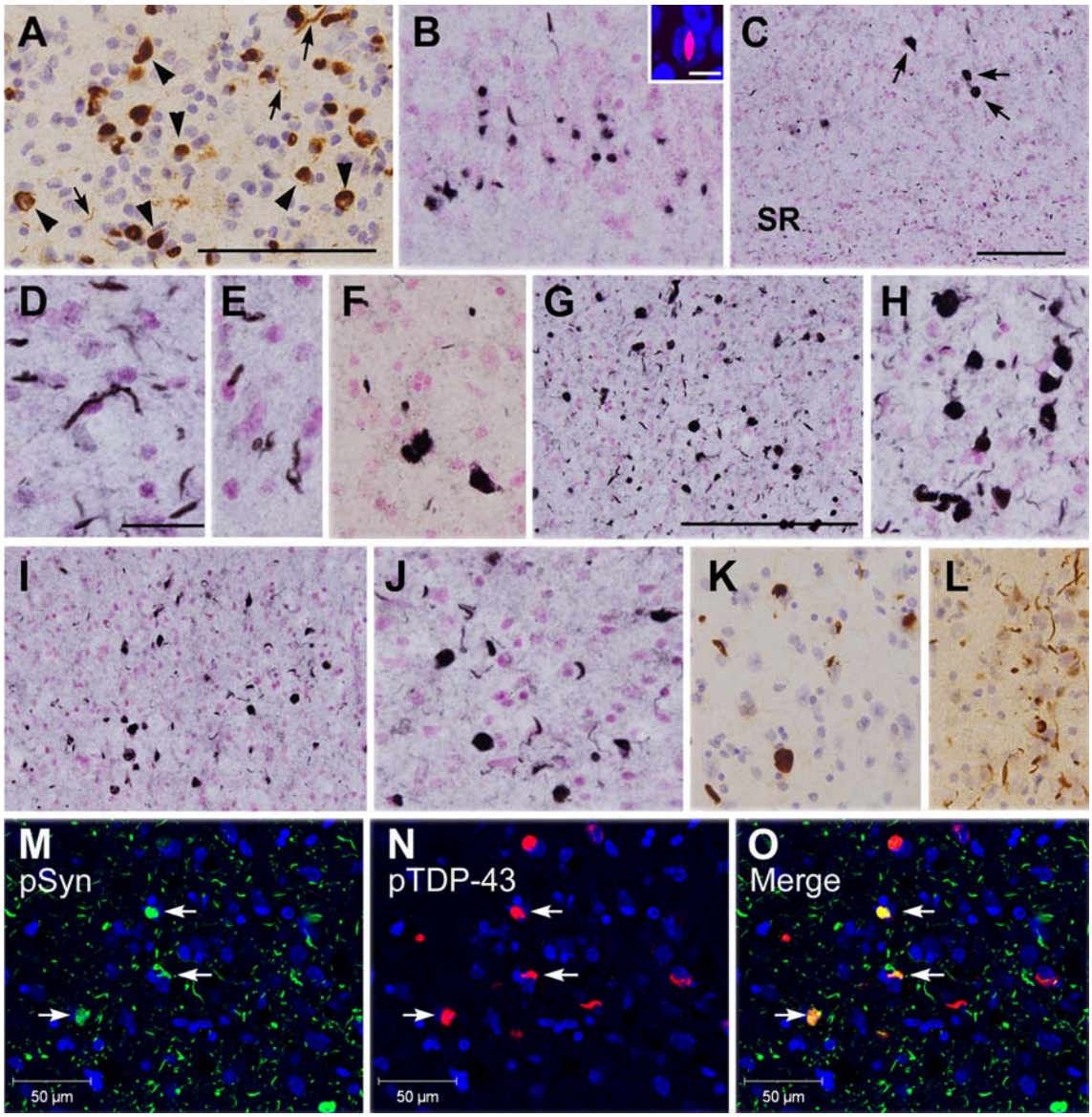

Fig. 2 Phosphorylated TDP-43 (*pTDP-43*) positive structures in cases of dementia with Lewy bodies. TDP-43 positive structures in cases of DLB plus AD with diffuse type of TDP-43 pathology are shown in **a**–**j**. Neuronal cytoplasmic inclusions (NCIs) and dystrophic neurites (DNs) in the entorhinal cortex of the pure DLB cases without AD pathology are shown in **k** (F-DLB7) and **l** (F-DLB8). **a** NCIs (*arrowheads*) and DNs (*arrows*) in amygdala. **b** NCIs in the dentate granule cells. *Inset* shows immunofluorescence staining of a lentiform inclusion (*red*) in the nucleus (*blue*) of a granule cell. **c** NCIs in the principal layer (*arrows*) and massive short threads-like structures in the stratum radiatum (*SR*) of the CA2/3 region. **d** A high power view of short threads-like structures in the stratum radiatum of the CA2/3 region. **e** Short threads-like structure in the alveus of the CA1 region. **f** Large NCIs and short neurites in the subiculum. **g** Massive NCIs and DNs in the superficial layer of the entorhinal cortex. **h** A high power view of NCIs and DNs in the entorhinal cortex. **i** Numerous NCIs and DNs in the superficial layer of the lateral occipitotemporal cortex. **j** A high power view of NCIs and DNs in the lateral occipitotemporal cortex. Double label immunofluorescence (**m**–**o**) shows partial co-localization of α-synuclein and pTDP-43 in the NCIs in the temporal neocortex (*arrows*), whereas most α-synuclein-positive neurites are negative for pTDP-43 (**m**–**o**). Immunostaining with pS403/404 (**a**, **i**, **j**) and pS409/410 (**b**–**h**, **k**, **l**). Double label immunofluorescence with anti-phosphorylated α-synuclein (pα#64) and pS403/404 (**m**–**o**). *Scale bars* **a**, **b**, **f**, **h**, **j**–**l** 100 µm; **d**, **e** 25 µm; **c**, **g**, **i** 200 µm; *inset* in **b** 10 µm

region, and that TDP-43 pathology in AD spreads from limbic structures to association cortices. In the present study, we observed amygdala only, limbic, and diffuse patterns of pTDP-43 pathology, not only in AD cases but also in DLB cases. These results suggest a common progressive anatomical pattern of pTDP-43 pathology in AD and DLB, with sequential spread from the amygdala to other limbic structures and then to association cortices. Although the number of cases was small, the results from our second series also suggests that there may be hierarchical involvement

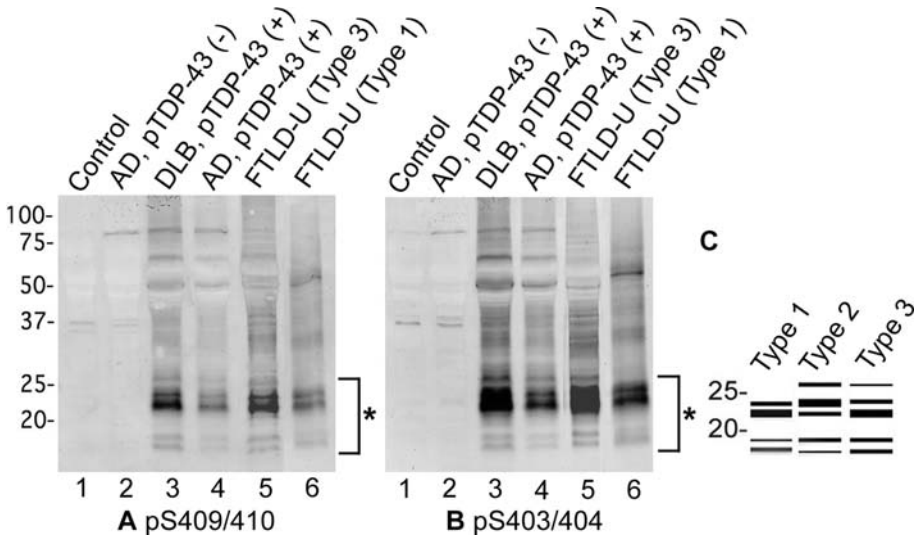

Fig. 3 The band pattern of the C-terminal fragments of phosphorylated TDP-43 (*pTDP-43*) in Alzheimer's disease (*AD*) and dementia with Lewy bodies (*DLB*). Immunoblot analyses of sarkosyl-insoluble, urea-soluble fractions, using phosphorylation-dependent anti-TDP-43 antibodies pS409/410 (**a**) and pS403/404 (**b**). *Lane 1* normal control; *lane 2* AD without pTDP-43 immunoreactivity (AD−); *lane 3* DLB with pTDP-43 immunoreactivity (DLB+); *lane 4* AD with pTDP-43 immunoreactivity (AD+); *lane 5* FTLD-U with Type 3 TDP-43 pathology; *lane 6* FTLD-U with Type 1 TDP-43 pathology. Schematic diagram (**c**) showing the band pattern of the C-terminal fragments of phosphorylated TDP-43 we have previously reported [14]. Strong immunoreactivity throughout the gel is observed only in DLB+ (*lane 3*), AD+ (*lane 4*) and FTLD-U (*lanes 5*, *6*). DLB+ (*lane 3*), AD+ (*lane 4*) and FTLD-U, Type 3 (*lane 5*) show similar patterns of low M_r bands with three major bands at 23, 24 and 26 kDa and two minor bands at 18 and 19 kDa, while FTLD-U, Type 1 (*lane 6*) shows two major bands at 23 and 24 kDa and two minor bands at 18 and 19 kDa (*asterisk*)

of neocortical regions, with the temporal association cortex involved first, followed by the frontal lobe and parietal lobe last.

Since subclassification of FTLD-U is based on TDP-43 pathology in the neocortex [7, 25, 35], only AD and DLB cases with the diffuse type of TDP-43 pathology could be subtyped. All of these cases had pTDP-43-positive NCIs and short DNs in the upper cortical layers, which corresponds to FTLD-U Type 3. In addition, most of them (8 of 9 AD cases and 2 of 3 DLB cases with the diffuse type) also had a few pTDP-43-positive NIIs in the dentate gyrus or the neocortex, These findings are consistent with the previous reports by Uryu et al. [39] and Nakashima-Yasuda et al. [30], but differ somewhat from Joseph et al. [19] who reported all three FTLD-U subtypes in AD, with the majority being Type 2.

Perhaps the greatest significance of this study is the evidence it provides that the pathological TDP-43 that accumulates in AD and DLB is similar to that in FTLD-U. First, positive staining of abnormal structures in immunohistochemistry and of abnormal bands on immunoblots of sarkosyl-insoluble fraction with pS403/404 and pS409/410 antibodies suggest that C-terminal phosphorylation sites of TDP-43 accumulated in AD and DLB brains are common to those in FTLD-U brains [14]. Second, intense staining of low-molecular-weight bands around 20–25 kDa on immunoblotting of sarkosyl-insoluble fraction from AD and DLB cases with neocortical pTDP-43 pathology indicates that the generation of C-terminal fragments of TDP-43 takes place in brains of these diseases as it does in FTLD-U [14, 18]. Furthermore, the band pattern of C-terminal fragments in AD and DLB corresponds to that of FTLD-U, Type 3, found in our previous report [14]. These findings suggest that there may be a common process that leads to the accumulation of pathological TDP-43 in FTLD-U Type 3, and some cases of AD and DLB. In this context, it should be noted that cases of familial FTLD-U with *PGRN* mutations always show Type 3 TDP-43 pathology [7]. Some familial FTLD-U cases with *PGRN* mutations have additional AD pathology [29] or tau and α-synuclein pathology [22]. Several mutations and polymorphisms of *PGRN* have recently been identified in AD and Parkinson's disease populations [5, 6] and these might underlie the co-occurrence of abnormal deposition of TDP-43, tau, and α-synuclein. Furthermore, a common genetic variant in *PGRN* (rs5848), located within a binding site for miR-659, has recently been identified as a major susceptibility factor for sporadic FTLD-U [34]. Homozygosity for the T-allele of rs5848 causes a significant reduction in the level of PGRN protein and is associated with a 3.2-fold increased risk of developing FTLD-U. The majority of these cases have Type 3 TDP-43 pathology. It is therefore possible that the subset of AD and DLB patients who develop TDP-43 pathology are carriers of this, or some other genetic risk factor, for TDP-43 proteinopathy. Partial colocalization of tau and TDP-43 or α-synuclein and TDP-43 in some cytoplasmic inclusions found in this

and other studies [1, 11, 13, 16, 30] may argue against a direct interaction between these proteins, and support the notion that there may be genetic or environmental factors that make the subset of neurons vulnerable for intracellular accumulation of tau, α-synuclein and TDP-43.

The fact that the accumulated TDP-43 in AD and DLB is biochemically similar to that believed to be pathogenic in FTLD-U, suggests that it might contribute to neurodegeneration or modify the clinical course. At present, there is a little data regarding the relationship between the presence of TDP-43 pathology and the clinical phenotype of AD or DLB. The older age at death of the AD cases with pTDP-43 pathology, observed in our second series (Table 4), is consistent with the previous report by Joseph et al. [19]. Nakashima-Yasuda et al. [30] also found a higher average age at death in the TDP-43 positive cases in Lewy body related diseases with dementia. A higher Braak NFT stage in the TDP-43 positive patients was found in DLB + AD cases by Nakashima-Yasuda et al. [30] and also in our first series of AD (Table 1). Further studies using larger cohorts with more detailed clinical, radiological and pathological data are needed to elucidate the clinical impact of TDP-43 pathology in AD and DLB.

Acknowledgments We thank Ms. H. Kondo, Ms. Y. Izumiyama, Ms. C. Haga and Ms. M. Luk for their excellent technical assistance. This research was supported by a Grant-in-Aid for Scientific Research (C) (to TA), a Grant-in-Aid for Scientific Research on Priority Areas—Research on Pathomechanisms of Brain Disorders (to MH), a Grant-in-Aid for Scientific Research (B) (to MH) from the Ministry of Education, Culture, Sports, Science and Technology of Japan, a grant from the Canadian Institutes of Health Research (grant # 74580) (to IM) and a grant from the Pacific Alzheimer Research Foundation (to IM).

References

1. Amador-Ortiz C, Lin WL, Ahmed Z et al (2007) TDP-43 immunoreactivity in hippocampal sclerosis and Alzheimer's disease. Ann Neurol 61:435–445. doi:10.1002/ana.21154
2. Arai T, Hasegawa M, Akiyama H et al (2006) TDP-43 is a component of ubiquitin-positive tau-negative inclusions in frontotemporal lobar degeneration and amyotrophic lateral sclerosis. Biochem Biophys Res Commun 351:602–611. doi:10.1016/j.bbrc.2006.10.093
3. Arai T, Ikeda K, Akiyama H et al (2003) Different immunoreactivities of the microtubule-binding region of tau and its molecular basis in brains from patients with Alzheimer's disease, Pick's disease, progressive supranuclear palsy and corticobasal degeneration. Acta Neuropathol 105:489–498
4. Baker M, Mackenzie IR, Pickering-Brown SM et al (2006) Mutations in progranulin cause tau-negative frontotemporal dementia linked to chromosome 17. Nature 442:916–919. doi:10.1038/nature05016
5. Brouwers N, Nuytemans K, van der Zee J et al (2007) Alzheimer and Parkinson diagnoses in progranulin null mutation carriers in an extended founder family. Arch Neurol 64:1436–1446. doi:10.1001/archneur.64.10.1436
6. Brouwers N, Sleegers K, Engelborghs S et al (2008) Genetic variability in progranulin contributes to risk for clinically diagnosed Alzheimer disease. Neurology 71:656–664. doi:10.1212/01.wnl.0000319688.89790.7a
7. Cairns NJ, Neumann M, Bigio EH et al (2007) TDP-43 in familial and sporadic frontotemporal lobar degeneration with ubiquitin inclusions. Am J Pathol 171:227–240. doi:10.2353/ajpath.2007.070182
8. Cruts M, Gijselinck I, van der Zee J et al (2006) Null mutations in progranulin cause ubiquitin-positive frontotemporal dementia linked to chromosome 17q21. Nature 442:920–924. doi:10.1038/nature05017
9. Davidson Y, Kelley T, Mackenzie IRA et al (2007) Ubiquitinated pathological lesions in frontotemporal lobar degeneration contain the TAR DNA-binding protein, TDP-43. Acta Neuropathol 113:521–533. doi:10.1007/s00401-006-0189-y
10. Feldman H, Levy AR, Hsiung GY et al (2003) A Canadian cohort study of cognitive impairment and related dementias (ACCORD): study methods and baseline results. Neuroepidemiology 22:265–274. doi:10.1159/000071189
11. Freeman SH, Spires-Jones T, Hyman BT, Growdon JH, Frosch MP (2008) TAR-DNA binding protein 43 in Pick disease. J Neuropathol Exp Neurol 67:62–67. doi:10.1097/nen.0b013e3181609361
12. Gitcho MA, Baloh RH, Chakraverty S et al (2008) TDP-43 A315T mutation in familial motor neuron disease. Ann Neurol 63:535–538. doi:10.1002/ana.21344
13. Hasegawa M, Arai T, Akiyama H et al (2007) TDP-43 is deposited in the Guam parkinsonism–dementia complex brains. Brain 130:1386–1394. doi:10.1093/brain/awm065
14. Hasegawa M, Arai T, Nonaka T et al (2008) Phosphorylated TDP-43 in frontotemporal lobar degeneration and amyotrophic lateral sclerosis. Ann Neurol 64:60–70. doi:10.1002/ana.21425
15. Higashi S, Iseki E, Yamamoto R et al (2007) Appearance pattern of TDP-43 in Japanese frontotemporal lobar degeneration with ubiquitin-positive inclusions. Neurosci Lett 419:213–218. doi:10.1016/j.neulet.2007.04.051
16. Higashi S, Iseki E, Yamamoto R et al (2007) Concurrence of TDP-43, tau and alpha-synuclein pathology in brains of Alzheimer's disease and dementia with Lewy bodies. Brain Res 1184:284–294. doi:10.1016/j.brainres.2007.09.048
17. Hu WT, Josephs KA, Knopman DS et al (2008) Temporal lobar predominance of TDP-43 neuronal cytoplasmic inclusions in Alzheimer disease. Acta Neuropathol 116:215–220. doi:10.1007/s00401-008-0400-4
18. Igaz LM, Kwong LK, Xu Y et al (2008) Enrichment of C-terminal fragments in TAR DNA-binding protein-43 cytoplasmic inclusions in brain but not in spinal cord of frontotemporal lobar degeneration and amyotrophic lateral sclerosis. Am J Pathol 173:182–194. doi:10.2353/ajpath.2008.080003
19. Josephs KA, Whitwell JL, Knopman DS et al (2008) Abnormal TDP-43 immunoreactivity in AD modifies clinicopathologic and radiologic phenotype. Neurology 70:1850–1857. doi:10.1212/01.wnl.0000304041.09418.b1
20. Kabashi E, Valdmanis PN, Dion P et al (2008) TARDBP mutations in individuals with sporadic and familial amyotrophic lateral sclerosis. Nat Genet 40:572–574. doi:10.1038/ng.132
21. Kosaka K (1990) Diffuse Lewy body disease in Japan. J Neurol 237:197–204. doi:10.1007/BF00314594
22. Leverenz JB, Yu CE, Montine TJ et al (2007) A novel progranulin mutation associated with variable clinical presentation and tau, TDP43 and alpha-synuclein pathology. Brain 130:1360–1374. doi:10.1093/brain/awm069
23. Lin WL, Dickson DW (2008) Ultrastructural localization of TDP-43 in filamentous neuronal inclusions in various neurodegenerative diseases. Acta Neuropathol 116:205–213. doi:10.1007/s00401-008-0408-9
24. Mackenzie IR, Bigio EH, Ince PG et al (2007) Pathological TDP-43 distinguishes sporadic amyotrophic lateral sclerosis from

amyotrophic lateral sclerosis with SOD1 mutations. Ann Neurol 61:427–434. doi:10.1002/ana.21147
25. Mackenzie IRA, Baborie A, Pickering-Brown S et al (2006) Heterogeneity of ubiquitin pathology in frontotemporal lobar degeneration: classification and relation to clinical phenotype. Acta Neuropathol 112:539–549. doi:10.1007/s00401-006-0138-9
26. Mackenzie IRA, Baker M, Pickering-Brown S et al (2006) The neuropathology of frontotemporal lobar degeneration caused by mutations in the progranulin gene. Brain 129:3081–3090. doi:10.1093/brain/awl271
27. McKeith IG, Dickson DW, Lowe J et al (2005) Diagnosis and management of dementia with Lewy bodies: third report of the DLB Consortium. Neurology 65:1863–1872. doi:10.1212/01.wnl.0000187889.17253.b1
28. Morita M, Al-Chalabi A, Anderson PM et al (2006) A locus on chromosome 9p confers susceptibility to ALS and frontotemporal dementia. Neurology 66:839–844. doi:10.1212/01.wnl.0000200048.53766.b4
29. Mukherjee O, Pastor P, Cairns NJ et al (2006) HDDD2 is a familial frontotemporal lobar degeneration with ubiquitin-positive tau-negative inclusions caused by a missense mutation in the signal peptide of progranulin. Ann Neurol 60:314–322. doi:10.1002/ana.20963
30. Nakashima-Yasuda H, Uryu K, Robinson J et al (2007) Co-morbidity of TDP-43 proteinopathy in Lewy body related diseases. Acta Neuropathol 114:221–229. doi:10.1007/s00401-007-0261-2
31. Neumann M, Kwong LK, Sampathu DM, Trojanowski JQ, Lee VM (2007) TDP-43 proteinopathy in frontotemporal lobar degeneration and amyotrophic lateral sclerosis: protein misfolding diseases without amyloidosis. Arch Neurol 64:1388–1394. doi:10.1001/archneur.64.10.1388
32. Neumann M, Sampathu DM, Kwong LK et al (2006) Ubiquitinated TDP-43 in frontotemporal lobar degeneration and amyotrophic lateral sclerosis. Science 314:130–133. doi:10.1126/science.1134108
33. Newell KL, Hyman BT, Growdon JH, Hedley-Whyte ET (1999) Application of the National Institute on Aging (NIA)–Reagan Institute criteria for the neuropathological diagnosis of Alzheimer disease. J Neuropathol Exp Neurol 58:1147–1155. doi:10.1097/00005072-199911000-00004
34. Rademakers R, Eriksen JL, Baker M et al (2008) Common variation in the miR-659 binding-site of GRN is a major risk factor for TDP43-positive frontotemporal dementia. Hum Mol Genet 17:3631–3642. doi:10.1093/hmg/ddn257
35. Sampathu DM, Neumann M, Kwong LK et al (2006) Pathological heterogeneity of frontotemporal lobar degeneration with ubiquitin-positive inclusions delineated by ubiquitin immunohistochemistry and novel monoclonal antibodies. Am J Pathol 169:1343–1352. doi:10.2353/ajpath.2006.060438
36. Schwab C, Arai T, Hasegawa M, Yu S, McGeer PL (2008) Colocalization of transactivation-responsive DNA-binding protein 43 and huntingtin in inclusions of Huntington disease. J Neuropathol Exp Neurol 67(12):1159–1165
37. Sreedharan J, Blair IP, Tripathi VB et al (2008) TDP-43 mutations in familial and sporadic amyotrophic lateral sclerosis. Science 319:1668–1672. doi:10.1126/science.1154584
38. Tan CF, Eguchi H, Tagawa A et al (2007) TDP-43 immunoreactivity in neuronal inclusions in familial amyotrophic lateral sclerosis with or without SOD1 gene mutation. Acta Neuropathol 113:535–542. doi:10.1007/s00401-007-0206-9
39. Uryu K, Nakashima-Yasuda H, Forman MS et al (2008) Concomitant TAR-DNA-binding protein 43 pathology is present in Alzheimer disease and corticobasal degeneration but not in other tauopathies. J Neuropathol Exp Neurol 67:555–564. doi:10.1097/NEN.0b013e31817713b5
40. Van Deerlin VM, Leverenz JB, Bekris LM et al (2008) TARDBP mutations in amyotrophic lateral sclerosis with TDP-43 neuropathology: a genetic and histopathological analysis. Lancet Neurol 7:409–416. doi:10.1016/S1474-4422(08)70071-1
41. Vance C, Al-Chalabi A, Ruddy D et al (2006) Familial amyotrophic lateral sclerosis with frontotemporal dementia is linked to a locus on chromosome 9p13.2–21.3. Brain 129:868–875. doi:10.1093/brain/awl030
42. Watts GDJ, Wymer J, Kovach MJ et al (2004) Inclusion body myopathy associated with Paget disease of bone and frontotemporal dementia is caused by mutant valosin-containing protein. Nat Genet 36:377–381. doi:10.1038/ng1332
43. Yokoseki A, Shiga A, Tan CF et al (2008) TDP-43 mutation in familial amyotrophic lateral sclerosis. Ann Neurol 63:538–542. doi:10.1002/ana.21392